

A New Algorithm for Optimizing Dubins Paths to Intercept a Moving Target

M. Akter *

M. M. Rizvi ✉[†]M. Forkan [‡]

October 30, 2023

Abstract

This paper is concerned with determining the shortest path for a pursuer aiming to intercept a moving target travelling at a constant speed. We introduce an intuitive and efficient mathematical model outlined as an optimal control problem to address this challenge. The proposed model is based on Dubins path where we concatenate two possible paths: a left-circular curve or a right-circular curve followed by a straight line. We develop and explore this model, providing a comprehensive geometric interpretation, and design an algorithm tailored to implement the proposed mathematical approach efficiently. Extensive numerical experiments involving diverse target positions highlight the strength of the model. The method exhibits a remarkably high convergence rate in finding solutions. For experiment purposes, we utilized the modelling software AMPL, employing a range of solvers to solve the problem. Subsequently, we simulated the obtained solutions using MATLAB, demonstrating the efficiency of the model in intercepting a moving target. The proposed model distinguishes itself by employing fewer parameters and making fewer assumptions, setting the model simplifies the complexities, and thus, makes it easier for experts to design optimal path plans.

Keywords. Dubins path, Optimal control problem, Path planning, Numerical methods.

*Department of Mathematics, University of Chittagong, Chittagong-4331, Bangladesh, email: masuda@cu.ac.bd,

[†]Centre for Smart Analytics (CSA), Institute of Innovation, Science and Sustainability, Federation University Australia, email: m.rizvi@federation.edu.au (corresponding author),

[‡]Department of Mathematics, University of Chittagong, Chittagong-4331, Bangladesh, email: forkan.math@cu.ac.bd

1 Introduction

Path planning for intercepting a moving target has been a significant challenge, demanding efficient strategies for path planning to ensure successful interception. This has applications in various domains such as robotics, aerospace, and military applications. The motivation behind the study of pursuer-target interception lies in real-world scenarios where one object needs to intersect with another. Researchers are exploring advanced algorithms, mathematical models, and artificial intelligence methods to enhance the accuracy and speed of interception. Our study focus deeply into the essential realm of pursuer-target interception path planning. By exploring innovative mathematical models and employing advanced computational techniques, our aim is to contribute significantly in this area. We propose efficient ways to minimize the pursuer's path when intercepting moving targets. Our research endeavors not only towards theoretical advancements but also practical solutions that can be universally applied, addressing the evolving challenges associated with intercepting moving targets in various domains.

Dubins [1] introduced the shortest path for vehicles moving only forward and turning in unidirectional turns (either left or right) from specific starting to ending positions on an in the 2D plane. The author described paths as combinations of curves and straight lines, where the vehicle starts and ends with a turn, and in the middle, it could be straight or curved. There are six possible combinations of these paths, represented by $D = \{LSL, RSL, RSR, LSR, LRL, RLR\}$, where L and R mean left and right turns, respectively. Reeds and Shepp [2] later expanded on Dubins work, allowing backward adaptability in these paths. Dubins results have since been further developed, incorporating geometric principles [3] and leveraging advanced theories in nonlinear optimal control [4]-[11]. Specifically, Pontryagin's Maximum Principle (PMP) [12] has been applied, enhancing the understanding and applications of Dubins paths. These developments have expanded the scope of Dubins work, making it a pivotal foundation in the study of optimal vehicle paths.

Numerous researchers have also been made an effort to develop a model to figure out the shortest distance for intercepting a moving target. Boissonnat and Bui's study [5] on the Relaxed Dubins Problem (RDP) focuses on finding the shortest Dubins path from a given configuration to a stationary target. Dubin's path problem from a fixed initial configuration to intercept a target have been extensively researched in several fields [13, 14]. When intercepting a moving target, researchers have also explored Dubins and relaxed Dubins optimal pathways [15]-[18]. Looker [19] proposes a search algorithm to determine the shortest *CS* type path for interception, assuming the pursuer behaves like a Dubins vehicle and the target moves at a constant speed. Meyer et al. [20] analyze problems related to minimum-time interception and interception at a predetermined time for a

target moving in a straight line. Additionally, Meyer et al. [21] address finding the shortest path for a Dubins vehicle without a terminal angle constraint, referred to as the 'relaxed Dubins' problem. In our research, we explore similar scenarios and attempt to reformulate various mathematical models for intercepting a moving target.

Moreover, Kaya [22] studied the reformulation of the Dubins path based on the optimality principle, aiming to find a time-optimal, collision-free trajectory for the Dubins vehicle. The author extended this approach to compute Dubins interpolating curves, which are the shortest curvature-constrained paths through a given sequence of points [23]. Zheng [24] introduced a model focusing on the Minimum-Time Intercept Problem (MTIP). This problem involves guiding a Dubins vehicle from a specific location with a specified initial heading angle to intercept a moving target in the shortest time possible. Later, the author discussed the same scenario with prescribed impact angle constraints [25]. Recently, Forkan et al. [26] introduced an innovative concept for effective path planning for a UAV, allowing optimal control of its heading during target touring. In this method, both the UAV and target are at the same altitude. The UAV's optimal path is determined using a nonlinear constrained model with an arc parameterization technique. This approach is further enhanced to tour a finite number of targets. In recent times, Hou [27] suggests a geometry-based impact time and angle control guiding rules without calculating the time-to-go that guarantees target captureability and zero terminal guidance command.

This paper proposes a geometric and mathematical model in Sections 3 and 4 to approximate the optimal path of the pursuer and the moving target. The suggested model is also suitable for minimizing the time it takes while a moving target is intercepted by a pursuer moving at a constant speed. The model is expected to have the following useful features:

- (i) When faced with a complex problem that involves numerous state and control variables, it's crucial for the method to provide approximations of optimal solutions. This is especially important in real-life applications where the problem-solving process can get increasingly intricate. The biggest hurdle in such scenarios is to develop an algorithm that can effectively and efficiently solve the problem which is the main motivation of this paper.
- (ii) The method should construct an algorithm to generate solutions efficiently at a reasonable computational time. Computational time management in our analysis is important because solving a large problem can be very costly.
- (iii) The methods should optimize the heading angles to determine the pursuer's direction to generate the shortest path of interception. This is an essential feature since it guarantees that, given those heading angles, one may optimize the pursuer's path or time without considering each of the feasible paths separately. Therefore, our

goal is to propose a mathematical model and increase its capacity for approximating the optimum trajectory in terms of length and time through the solution of a mathematical model.

We are therefore interested in learning more about how the suggested models might construct the optimum path with minimal computational effort. The strengths and along with advantages of the proposed method with features (i)-(iii) are illustrated through the examples in Section 6 and the findings are demonstrated in Figures (3-7).

The rest of this paper comprises the following sections. In Section 2, we illustrate reformulation of Dubins problem as a time-optimal control problem and Pontryagin's Maximum Principle. The geometrical interpretation of optimal path planning of a pursuer for intercepting a moving target is described in Section 3. In Section 4, the model for finding an optimal path of the pursuer to intercept a moving target is proposed. In Section 5, we introduce an algorithm to implement the proposed model. Numerical experiments are conducted and we provide the results and discussions based on numerical experiments in Section 6. The last section presents the conclusion of the paper.

2 Formulation of Optimal Control Problem

In this section, the optimal control problem for the pursuer and moving target interception is formulated and control law is discussed using Pontryagin's Maximum Principle.

Let us consider the optimum path, denoted as $z(t) : [t_0, t_f] \rightarrow \mathbb{R}^2$, starting from the initial position to the interception point. This path $z(t)$ measure the entire travel path for both the pursuer and the target until they meet each other. We assume that the target is moving in a straight line with a constant speed and the pursuer does not face any obstacles during the motion. We also assume that the pursuer can not reverse its direction to intercept a target. The pursuer also has complete knowledge of the target's future trajectory and speed.

We consider $(x(t), y(t)) \in \mathbb{R}^2$ along $z(t)$ with $\dot{x}(t) = |\mathbf{V}| \cos \theta(t)$ and $\dot{y}(t) = |\mathbf{V}| \sin \theta(t)$, where $\theta(t)$ is the heading angle, which is measured from the x -axis through counterclockwise and $\theta(t) \in [0, 2\pi]$, $|\mathbf{V}|$ is the speed, R is the minimum turning radius of the pursuer.

Let $t \in [t_0, t_f]$, where t_f be the terminal time which is unknown and needs to be determined, and t_0 be the initial time. Therefore, the minimum path of the pursuer for intercepting a moving target is determined by the arc length functional

$$\int_{t_0}^{t_f} \sqrt{\dot{x}^2 + \dot{y}^2} dt = \int_{t_0}^{t_f} \|\dot{z}(t)\| dt = |\mathbf{V}|(t_f - t_0), \quad (1)$$

where, $\|\dot{z}(t)\| = |\mathbf{V}|$, $\dot{z}(t) = \frac{dz}{dt}$, and $\|\cdot\|$ is the Euclidean norm.

Furthermore, the unit tangent vector is defined by $T(t) = \frac{\dot{z}(t)}{\|\dot{z}(t)\|} = (\cos \theta(t), \sin \theta(t))$, and the curvature at each point of the path is calculated as $a = \frac{\|\dot{T}(t)\|}{\|\dot{z}(t)\|} = \frac{|\dot{\theta}(t)|}{|\mathbf{V}|}$.

The quantity $\frac{\dot{\theta}(t)}{|\mathbf{V}|}$ can be positive or negative, and referred to as the signed curvature. If $\dot{\theta}(t) > 0$ then the pursuer moves in the counter-clockwise direction (left turns (L)) and if $\dot{\theta}(t) < 0$ then the pursuer moves in the clockwise direction (right turns (R)), and also $\dot{\theta}(t) = 0$, if the pursuer moves in the straight line (S). Let $u(t) = \frac{\dot{\theta}(t)}{|\mathbf{V}|}$.

Let us consider that heading angles of pursuer at the starting position $P(x_{P_0}, y_{P_0})$ is θ_{P_0} , and the constant velocities of pursuer and target are \mathbf{V}_P and \mathbf{V}_T respectively.

Hence the optimal control problem can be formulated as follows.

$$\begin{aligned} \min \quad & f = \int_{t_0}^{t_f} |\mathbf{V}_P| dt = |\mathbf{V}_P|(t_f - t_0). \\ \text{subject to} \quad & \dot{x}_P(t) = |\mathbf{V}_P| \cos \theta_P(t), \quad x_P(t_0) = x_{P_0}, \\ & \dot{y}_P(t) = |\mathbf{V}_P| \sin \theta_P(t), \quad y_P(t_0) = y_{P_0}, \\ & \dot{\theta}_P(t) = u(t)|\mathbf{V}_P|, \quad \theta_P(t_0) = \theta_{P_0}, \\ & |u(t)| \leq a, \end{aligned} \tag{2}$$

where $(x_P(t), y_P(t), \theta_P(t))$ and $(x_T(t), y_T(t), \theta_T)$ are represent the positions along the paths of pursuer and moving target, respectively.

Let's consider that the target is moving with constant speed $|\mathbf{V}_T| > 0$ without making any turns or maneuvers. The direction of the target's movement is indicated by θ_T , which falls within the range of $[0, 2\pi]$. Since the target does not change its direction, the value of θ_T remains fixed throughout the engagement. Assuming the target's initial position is (x_{T_0}, y_{T_0}) , its position at any time $t \geq 0$ can be expressed as follows:

$$\begin{aligned} \dot{x}_T(t) &= |\mathbf{V}_T| \cos \theta_T, \quad x_T(t_0) = x_{T_0}, \\ \dot{y}_T(t) &= |\mathbf{V}_T| \sin \theta_T, \quad y_T(t_0) = y_{T_0}. \end{aligned} \tag{3}$$

2.1 Pontryagin's Maximum Principle

In this subsection, we will state the necessary conditions of optimality by Pontryagin's maximum principle [12] for Problem (2) to obtain the optimal path for intercepting a target by a pursuer.

Define the Hamiltonian function for Problem (2) as follows.

$$H(x_P(t), y_P(t), \theta_P(t), \mu_0, \mu_1(t), \mu_2(t), \mu_3(t), u(t)) = \mu_0 |\mathbf{V}_P| + \mu_1(t) |\mathbf{V}_P| \cos \theta_P(t) + \mu_2(t) |\mathbf{V}_P| \sin \theta_P(t) + \mu_3(t) u(t) |\mathbf{V}_P|, \quad (4)$$

where μ_0 is a scalar parameter and $\mu_i : [t_0, t_f] \in \mathbb{R}, i = 1, 2, 3$, are the costate variables. The costate variables are required to satisfy

$$\dot{\mu}_1(t) = -H_{x_P}(t) = 0, \quad (5)$$

$$\dot{\mu}_2(t) = -H_{y_P}(t) = 0, \quad (6)$$

$$\dot{\mu}_3(t) = -H_{\theta_P}(t) = \mu_1(t) |\mathbf{V}_P| \sin \theta_P(t) - \mu_2(t) |\mathbf{V}_P| \cos \theta_P(t). \quad (7)$$

In addition to (5)-(7), one has $\dot{x}_P(t) = H_{\mu_1}(t)$, $\dot{y}_P(t) = H_{\mu_2}(t)$, $\dot{\theta}_P(t) = H_{\mu_3}(t)$. Note that from (5) and (6), we have that $\mu_1(t) = \bar{\mu}_1$, $\mu_2(t) = \bar{\mu}_2$ for all $t \in [t_0, t_f]$, where $\bar{\mu}_1$ and $\bar{\mu}_2$ are constants.

In addition to the state differential equations and other constraints given in (2) and the adjoint differential equations (5) - (7), the following conditions hold:

$$u(t) \in \arg \min_{\|w\| \leq a} H(x_P(t), y_P(t), \theta_P(t), \mu_0, \mu_1(t), \mu_2(t), \mu_3(t), w), \quad (8)$$

$$H(t) = 0. \quad (9)$$

Thus, using (4), equation (8) can be written more simply as,

$$u(t) \in \arg \min_{\|w\| \leq a} \mu_3(t) w, \quad (10)$$

therefore minimizing the Hamiltonian function yields the following control law.

$$u(t) = \begin{cases} a, & \text{if } \mu_3(t) < 0 \\ -a, & \text{if } \mu_3(t) > 0 \\ \text{undetermined,} & \text{if } \mu_3(t) = 0. \end{cases} \quad (11)$$

3 Interception of Pursuer and Moving Target: A Geometric Perspective

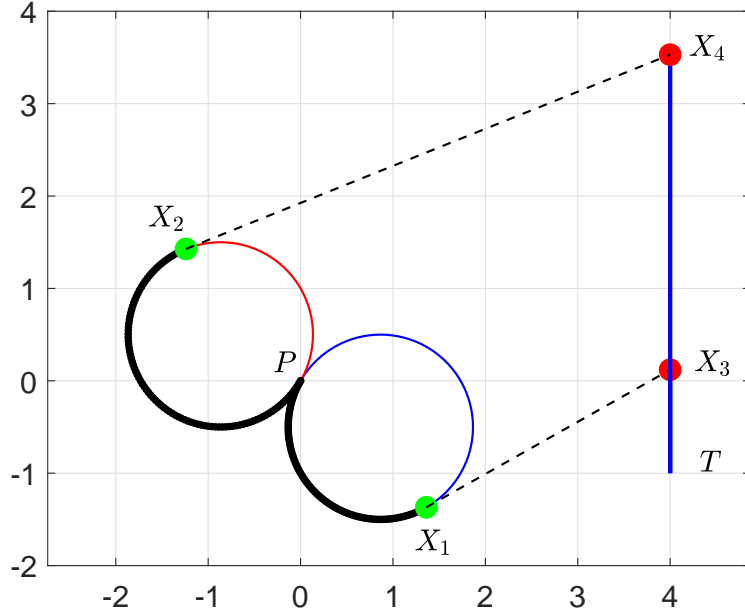


Figure 1: Feasible optimal paths of interception of moving target and a pursuer.

This section illustrates path planning for a pursuer intercepting a target, where the pursuer and target are moving at constant speeds in two dimensions. The geometric interpretation for constructing the paths of a pursuer intercepting a moving target is demonstrated below.

Let the pursuer and the target initiate their journey from the points $P(x_{P_0}, y_{P_0}, \theta_{P_0})$ and $T(x_{T_0}, y_{T_0}, \theta_{T_0})$, respectively and after certain period of time the pursuer intersect the target at a arbitrary unknown position. Following Dubin's path the pursuer adheres to a minimum turning radius, allowing it the flexibility to make left or right turns to optimize its path. According to Figure 1, the pursuer can follow either path PX_1 or PX_2 to travel across a circular trajectory. Subsequently, based on its choice of the left or right turn, the pursuer follows a straight-line path, either X_1X_3 or X_2X_4 , with the aim of intercepting the moving target, while maintaining a constant speed of $|\mathbf{V}_P|$. Simultaneously, the target is in motion at a constant speed of $|\mathbf{V}_T|$, moving towards its path. It is assumed that after a certain time interval t , both the pursuer and the target will intersect at a point denoted as X_3 or X_4 . To ensure the success of these intercepts, we make the assumption that the

pursuer's speed, $|\mathbf{V}_P|$, exceeds that of the target, $|\mathbf{V}_T|$. This creates two possible feasible paths of the type $CS + S_T$ (C-curve and S-st. line) which are as follows:

$$CS + S_T \equiv \begin{cases} LS + S_T \equiv \text{arc } PX_1 + \text{st. line } X_1X_3 + \text{st. line } TX_3, & \text{or,} \\ RS + S_T \equiv \text{arc } PX_2 + \text{st. line } X_2X_4 + \text{st. line } TX_4, \end{cases} \quad (12)$$

4 Mathematical Model for Intercepting a Moving Target

In this section, we present a mathematical model to determine the most efficient path for a pursuer to intercept a moving target. According to the geometrical interpretation outlined in Section 3, we formulate mathematical expressions to calculate the concatenated lengths. These lengths comprise two sub-paths, each involving a combination of the CS type and S_T . Moreover, the optimal path intercepting a moving target falls into one of the two specific cases detailed in the following set discussed in (12).

$$\{LS + S_T, RS + S_T\}. \quad (13)$$

Let us assume an initial time $t_0 = 0$ and a terminal time $t_f = t_3$ for the pursuer, so that the length of each sub-path can be defined as $\xi_i = |\mathbf{V}_P|(t_i - t_{i-1})$, where $i = 1, 2, 3$. Additionally, assuming the starting time for the target $t_4 = t_0 = 0$ and the time it gets intercepted by the pursuer is $t_f = t_3$. The notation $\xi_i = |\mathbf{V}_T|(t_{i-1} - t_i)$, where $i = 4$ represents the distance traveled by the target until it is intercepted by the pursuer. Now we solve the ordinary differential equations given in (2) for $x_P(t)$, $y_P(t)$, $\theta_P(t)$ with the interval $t_{i-1} \leq t \leq t_i$, $i = 1, 2, 3$ yields,

$$\begin{aligned} \int_{t_{i-1}}^{t_i} \dot{x}_P(t) dt &= \int_{t_{i-1}}^{t_i} |\mathbf{V}_P| \cos \theta_P(t) dt, \\ \int_{t_{i-1}}^{t_i} \dot{y}_P(t) dt &= \int_{t_{i-1}}^{t_i} |\mathbf{V}_P| \sin \theta_P(t) dt, \\ \int_{t_{i-1}}^{t_i} \dot{\theta}_P(t) dt &= \int_{t_{i-1}}^{t_i} |\mathbf{V}_P| u(t) dt. \end{aligned} \quad (14)$$

From (14), we obtain the position $(x_P(t_i), y_P(t_i))$, $i = 1, 2$ along turning curve (C) yields

$$\begin{aligned}
x_P(t_i) &= x_P(t_{i-1}) + (\sin \theta_P(t_i) - \sin \theta_P(t_{i-1})) / (\dot{\theta}_P(t) / |\mathbf{V}_P|), \\
y_P(t_i) &= y_P(t_{i-1}) - (\cos \theta_P(t_i) - \cos \theta_P(t_{i-1})) / (\dot{\theta}_P(t) / |\mathbf{V}_P|),
\end{aligned} \tag{15}$$

where

$$\frac{\dot{\theta}_P(t)}{|\mathbf{V}_P|} = \begin{cases} a & \text{if } \dot{\theta}_P(t) > 0 \\ -a & \text{if } \dot{\theta}_P(t) < 0 \\ 0 & \text{if } \dot{\theta}_P(t) = 0, \end{cases} \tag{16}$$

The position $(x_P(t_i), y_P(t_i))$, with $i = 3$ at which the pursuer intercepts the moving target along a straight line (S) can be described as

$$\begin{aligned}
x_P(t_i) &= x_P(t_{i-1}) + |\mathbf{V}_P| \cos \theta_P(t_{i-1})(t_i - t_{i-1}), \\
y_P(t_i) &= y_P(t_{i-1}) + |\mathbf{V}_P| \sin \theta_P(t_{i-1})(t_i - t_{i-1}).
\end{aligned} \tag{17}$$

Since the speed of the pursuer ($|\mathbf{V}_P|$) is constant over the time duration $[t_i - t_{i-1}]$, $i = 3$, so the length of straight path for pursuer can be written as

$$\xi_i = |\mathbf{V}_P|(t_i - t_{i-1}), \quad i = 3. \tag{18}$$

Now using (18), we rewrite (17) as below:

$$\begin{aligned}
x_P(t_i) &= x_P(t_{i-1}) + \xi_i \cos \theta_P(t_{i-1}), \\
y_P(t_i) &= y_P(t_{i-1}) + \xi_i \sin \theta_P(t_{i-1}),
\end{aligned} \tag{19}$$

and heading angles of pursuer along the both curve (C) and straight line (S) can be obtained as

$$\theta_P(t_i) = \theta_P(t_{i-1}) + (\dot{\theta}_P(t) / |\mathbf{V}_P|) |\mathbf{V}_P| (t_i - t_{i-1}), \quad i = 1, 2, \tag{20}$$

where $(\dot{\theta}_P(t) / |\mathbf{V}_P|) = a$, for left-turn circular arc, $(\dot{\theta}_P(t) / |\mathbf{V}_P|) = -a$, for right-turn circular arc and $(\dot{\theta}_P(t) / |\mathbf{V}_P|) = 0$, for straight line.

Using (15), (16), and (19), the optimum path CS of the pursuer for the time duration from t_0 to t_3 is given below.

$$x_P(t_3) - x_P(t_0) = \frac{1}{a} (-\sin \theta_P(t_0) + 2 \sin \theta_P(t_1) - \sin \theta_P(t_2)) + \xi_3 \cos \theta_P(t_2), \tag{21}$$

and

$$y_P(t_3) - y_P(t_0) = \frac{1}{a}(\cos \theta_P(t_0) - 2 \cos \theta_P(t_1) + \cos \theta_P(t_2)) + \xi_3 \sin \theta_P(t_2). \quad (22)$$

Now, we calculate the target path for the time duration from t_4 ($t_4 = t_0 = 0$) to t_3 as below,

$$\int_{t_0}^{t_3} \dot{x}_T(t) dt = \int_{t_0}^{t_3} |\mathbf{V}_T| \cos \theta_T dt,$$

and

$$\int_{t_0}^{t_3} \dot{y}_T(t) dt = \int_{t_0}^{t_3} |\mathbf{V}_T| \sin \theta_T dt,$$

By simplification the above relations and using $\xi_4 = |\mathbf{V}_T|(t_3 - t_0)$, we obtain the path for moving target as

$$x_T(t_3) - x_T(t_0) = \xi_4 \cos \theta_T, \quad (23)$$

and

$$y_T(t_3) - y_T(t_0) = \xi_4 \sin \theta_T. \quad (24)$$

It is note that when a moving target is intercepted by the pursuer, their positions coincide. In other words, $(x_P(t_3), y_P(t_3)) = (x_T(t_3), y_T(t_3))$ at the interception moment. As a result combining (21)-(24) and thus we obtain,

$$x_P(t_0) - x_T(t_0) + \frac{1}{a}(-\sin \theta_P(t_0) + 2 \sin \theta_P(t_1) - \sin \theta_P(t_2)) + \xi_3 \cos \theta_P(t_2) - \xi_4 \cos \theta_T = 0, \quad (25)$$

and

$$y_P(t_0) - y_T(t_0) + \frac{1}{a}(\cos \theta_P(t_0) - 2 \cos \theta_P(t_1) + \cos \theta_P(t_2)) + \xi_3 \sin \theta_P(t_2) - \xi_4 \sin \theta_T = 0. \quad (26)$$

Since the pursuer and target move with separate constant velocities and intercept to each other at the same moment, we must include an additional constraint to the optimization problem as

$$|\mathbf{V}_T| \sum_{i=1}^3 \xi_i - |\mathbf{V}_P| \xi_4 = 0. \quad (27)$$

Considering equations (20) and (25)-(27), we can formulate the following mathematical model for target interception.

$$\begin{aligned}
& \min \quad f = \sum_{i=1}^4 \xi_i \\
& \text{subject to} \\
& x_P(t_0) - x_T(t_0) + \frac{1}{a} (-\sin \theta_P(t_0) + 2 \sin \theta_P(t_1) - \sin \theta_P(t_2)) + \xi_3 \cos \theta_P(t_2) - \xi_4 \cos \theta_T = 0, \\
& y_P(t_0) - y_T(t_0) + \frac{1}{a} (\cos \theta_P(t_0) - 2 \cos \theta_P(t_1) + \cos \theta_P(t_2)) + \xi_3 \sin \theta_P(t_2) - \xi_4 \sin \theta_T = 0, \\
& |\mathbf{V}_T|(\xi_1 + \xi_2 + \xi_3) - |\mathbf{V}_P|\xi_4 = 0, \\
& \xi_i \geq 0, \quad i = 1, 2, 3, 4,
\end{aligned} \tag{28}$$

where

$$\theta_{P_1} = \theta_{P_0} + a\xi_1, \quad \theta_{P_2} = \theta_{P_1} - a\xi_2.$$

5 Proposed Optimal Path Algorithm

The possible pathways that described in (28) intersect a moving target satisfy the minimum turn radius criteria established in the following Proposition (5.1).

Proposition 5.1 *A target cannot be intercepted by the pursuer while it is inside its turning circle.*

Proof. Let C be the centre of the pursuer's turning circle, and the pursuer's position $P(t)$ before leaving the turning circle is $P(t_2)$. We assume that the pursuer and the target intercept at point $T(t_3)$. The radius of turning circle is PC that perpendicular to the tangent PT and CT is the hypotenuse of the triangle TPC . Therefore, from Figure-2 we have $PT = \sqrt{TC^2 - PC^2}$. Since $TC^2 - PC^2 \geq 0$ and $PC \geq 0$, it implies that the target's distance from the center of the turning circle is always greater or equal to the radius of the pursuer's turning circle. \square

Now we present the algorithm that implements our proposed model (28) to find the best path for a pursuer intercepting a moving target. In Step 2 of the algorithm, we minimize (28) using specified inputs: curvature a , and speeds $|\mathbf{V}_P|$ and $|\mathbf{V}_T|$ for pursuer and target, respectively. The optimal solution determines the lengths of the pursuer's left or right circular paths, along with the straight line from the circular path's exit point to the target intersection point. Using these lengths, we calculate the time required for each of those sections of the paths.

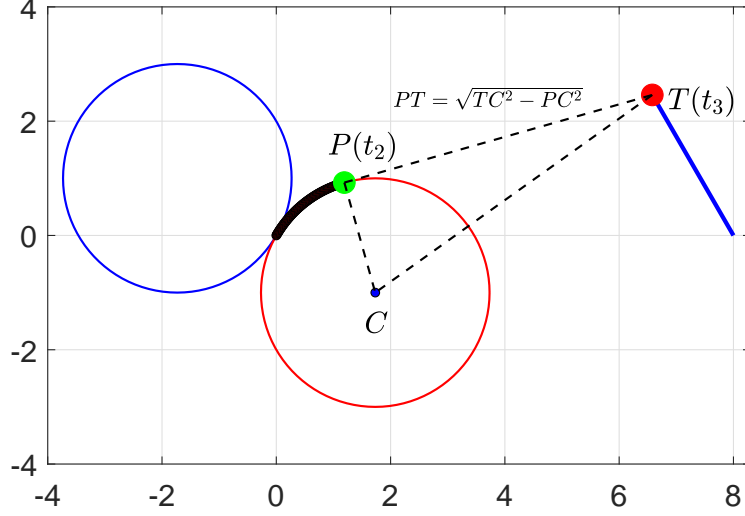


Figure 2: Area where pursuer can not intercept target.

In Step (3) of the algorithm, we utilize the output obtained in Step (2) to determine the positions of both pursuer and target trajectories at time $t \in [t_o, t_f]$. Initially, in Step (3)(a), we locate the center of the turning radius circle of the pursuer, a necessary step for visualizing the turning curves. Subsequently, in Step (3)(b)(i) and (ii), we compute the positions (x, y) of both the target and pursuer from their starting points up until the intercept occurs.

Algorithm 5.1 Step 1 (Input)

Choose initial positions $P(x_{P_0}, y_{P_0}, \theta_{P_0})$ and $T(x_{T_0}, y_{T_0}, \theta_{T_0})$ for a pursuer and a target respectively. Set turning radius R , curvature $a = \frac{1}{R}$, and speeds $|\mathbf{V}_P|$ and $|\mathbf{V}_T|$. Define variables $\xi_i, i = 1, \dots, 4$.

Step 2 (Determine the length from pursuer's initial point to intercept point)

Let left turn angle $\theta_{P_1} = \theta_{P_0} + a\xi_1$ and right turn angle $\theta_{P_2} = \theta_{P_1} - a\xi_2$.

Find $\xi := (\bar{\xi}_1, \bar{\xi}_2, \bar{\xi}_3, \bar{\xi}_4)$ that solves Model (28).

Set $\bar{F} := [\bar{\xi}_1, \bar{\xi}_2, \bar{\xi}_3, \bar{\xi}_4]$. Set $\bar{T} := [\bar{t}_1, \bar{t}_2, \bar{t}_3, \bar{t}_4]$, where $\bar{t}_i = \bar{\xi}_i / |\mathbf{V}_P|, i = 1, 2, 3,$

$\bar{t}_4 = \bar{\xi}_4 / |\mathbf{V}_T|$ and $f = \sum_{i=1}^4 \bar{\xi}_i$.

Step 3 (Simulation)

(a) (Determining turning circle centers)

Set centers for left-turn circle (α_L, β_L) and right-turn circle (α_R, β_R) where

$$\alpha_L, \alpha_R = x_{P_0} \pm R \sin \theta_{P_0},$$

and

$$\beta_L, \beta_R = y_{P_0} \pm R \cos \theta_{P_0}.$$

(b) (Generating points along the path)

Calculate $\theta_{P_1} = \theta_{P_0} + a\bar{\xi}_1$ and $\theta_{P_2} = \theta_{P_1} - a\bar{\xi}_2$.

(i) (Points along target trajectory)

St line: Set $\hat{t}_0 = t_0$ and $j = 1, \dots, k$.

$$\hat{t}_j := \hat{t}_{j-1} + (\bar{t}_4 - t_0)/k,$$

$$x_{T_j} = x_T + |\mathbf{V}_T| \cos(\theta_T)(\bar{t}_j - t_0),$$

and

$$y_{T_j} = y_T + |\mathbf{V}_T| \sin(\theta_T)(\bar{t}_j - t_0).$$

Set $\bar{X}_1 = [x_{T_j}, y_{T_j}]$.

(ii) (Points along pursuer trajectory)

Left-turn: Set $\theta_{P_0} = \theta_{P_0}$ and $i = 1, \dots, m$.

$$\bar{\theta}_{P_i} := \bar{\theta}_{P_{i-1}} + (\theta_{P_1} - \theta_{P_0})/m,$$

$$x_{P_i} = x_{P_0} + (\sin(\bar{\theta}_{P_i}) - \sin(\theta_{P_0}))/a,$$

and

$$y_{P_i} = y_{P_0} - (\cos(\bar{\theta}_{P_i}) - \cos(\theta_{P_0}))/a.$$

Set $\bar{X}_2 = [x_{P_i}, y_{P_i}]$.

Right-turn: Set $\hat{\theta}_{P_0} = \theta_{P_0}$ and $i = 1, \dots, m$.

$$\hat{\theta}_{P_i} := \hat{\theta}_{P_{i-1}} + (\theta_{P_2} - \theta_{P_0})/m,$$

$$x_{P_i} = x_{P_0} - (\sin(\hat{\theta}_{P_i}) - \sin(\theta_{P_0}))/a,$$

and

$$y_{P_i} = y_{P_0} + (\cos(\hat{\theta}_{P_i}) - \cos(\theta_{P_0}))/a.$$

Set $\bar{X}_3 = [x_{P_i}, y_{P_i}]$.

St. Line: Use (19) and similar steps stated in Step (b)(i).

Set $\bar{X}_4 = [x_{P_i}, y_{P_i}]$.

Step 4 (Output)

Target trajectory \bar{X}_1 and Pursuer trajectory $\bar{X}_2 \cup \bar{X}_3 \cup \bar{X}_4$.

6 Numerical Experiments, Results and Analysis

In this section, we present the results obtained from the numerical experiments to validate the efficiency of our proposed model (28) for determining the optimal path for a pursuer to intercept a moving target. We provide initial locations and heading angles for both the pursuer and the target, considering their constant velocities, in order to calculate the optimal path for target interception.

In Example 1, we tested our proposed Algorithm (5.1) with various combinations of pursuer and target positions, velocities, and turning radii. The pursuer’s objective was to intercept the target in the shortest possible distance or time. As the turning radius is influenced by both angular and linear speeds, Example 2 tested the model, calculating the turning radius using these parameters. We explored different optimal path combinations by adjusting angular speeds, both increasing and decreasing them, to evaluate their impact on interception strategies. In experiments conducted in Examples 1 and 2, Algorithm (5.1) demonstrated remarkable efficiency in computing optimal paths, as evidenced by Figures 3–7 and the detailed results presented in Tables 1-5.

In the experiments, we implement Algorithm (5.1) writing codes in AMPL [28], utilizing various solvers such as Ipopt [29] and KNITRO [30], all with default settings, to solve the problems. Almost both solvers exhibited a high convergence rate in solving our model. The obtained solutions are simulated by using MATLAB for the numerical experiments. In our analysis, the computations are conducted on an HP Evo laptop with 16 GB RAM and a Core i7 processor running at 4.6 GHz.

Example 1

Let an initial position for the pursuer, denoted as $P(0, 0, 2\pi/3)$ and a target point $T(-5, 0, \pi/2)$. The objective is for the pursuer P , moving at a constant speed $|\mathbf{V}_P|$, to intercept the target T , which is also moving at a constant speed $|\mathbf{V}_T|$. This interception is accomplished by finding the shortest path f , as determined by Algorithm (5.1). It is important to note that we assume a minimum turning radius of $R = 1$ for the pursuer’s turning curve. The pursuer takes time t to intercept the target.

The results of our analysis reveal that the $LS + S_T$ path proves to be the optimal choice to successfully achieve the task, as illustrated in Figure 3(a). Another feasible path is the $RS + S_T$ path, showcased in Figure 3(b). Table 1 provides a detailed breakdown of the lengths and time periods associated with each section of these paths. Specifically, the total length of the path obtained by our algorithm $f = 6.26$, and the corresponding time is $t = 1.04$. In particular, the non-optimal path requires two times more length, ($f = 14.16$) and time ($t = 2.36$) when compared to the optimal path, as illustrated in Table 1 and demonstrated in Figure 3(a) and (b). The computational time taken by our system to

derive the optimum path is around 0.078 seconds.

Table 1: *Model Performance Variations for Optimal Path Generations.*

$ \mathbf{V} - R$	Length				Time					
$ \mathbf{V}_P = 5$ $ \mathbf{V}_T = 1$ $R = 1$	Left turn $\bar{\xi}_1$	Right turn $\bar{\xi}_2$	St. line $\bar{\xi}_3$	Target St. line $\bar{\xi}_4$	Left turn \bar{t}_1	Right turn \bar{t}_2	St. line \bar{t}_3	Target St. line \bar{t}_4	Total value f	Total value t
Optimal Path	0.92	0	4.30	1.04	0.18	0	0.86	1.04	6.26	1.04
Feasible Path	0	5.70	6.09	2.36	0	1.14	1.21	2.36	14.16	2.36

Now, we fixed the target point to the right side of the pursuer, specifically to coordinates $T(8, -2, 2\pi/3)$, while increasing the target’s speed to $|\mathbf{V}_T| = 2$. Additionally, we adjusted the initial angle of the pursuer to $\pi/3$. The pursuer’s turning curve meets a minimum radius of $R = 1$.

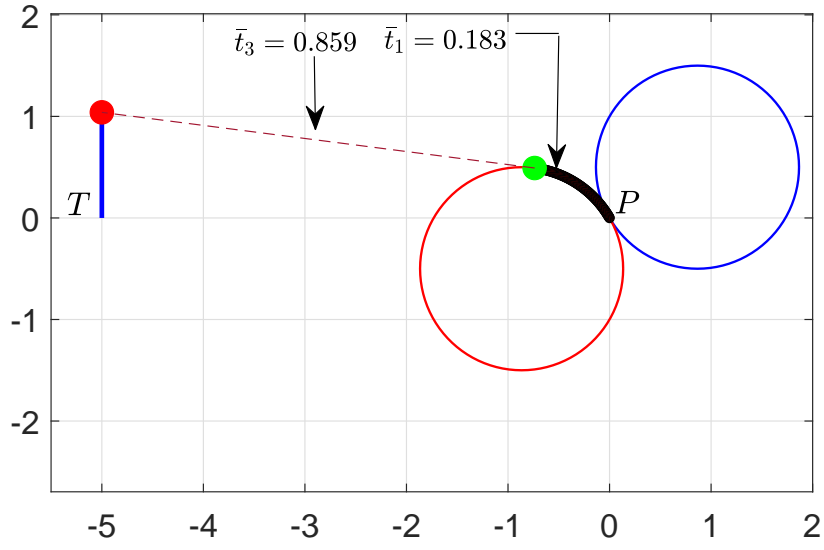
Our analysis concluded that the optimal choice to successfully achieve this task is the $RS + S_T$ path, as shown in Figure 4(a). Other feasible path is $LS + S_T$, displayed in Figure 4(b). Table 2 provides a comprehensive breakdown of the lengths and time intervals associated with each section of these paths. Specifically, our algorithm yielded an optimal path length of $f = 9.55$ and a corresponding time of $t = 1.36$. Almost the previous analysis, the non-optimal path requires twice the length and time compared to the optimal path, as depicted in Figure 4(a) and (b). The computational time needed for our system to determine the optimal path is around 0.093 seconds.

Table 2: *Model Performance Variations for Optimal Path Generations.*

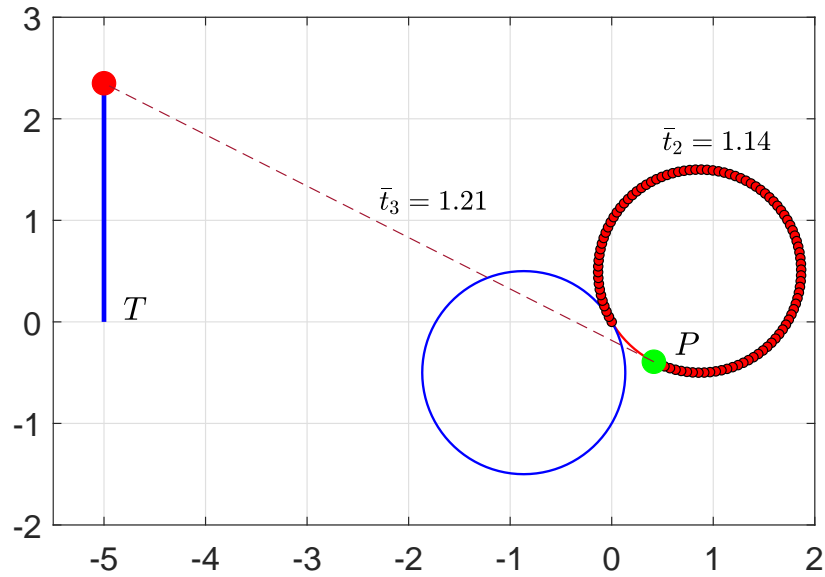
$ \mathbf{V} - R$	Length				Time					
$ \mathbf{V}_P = 5$ $ \mathbf{V}_T = 2$ $R = 1$	Left turn $\bar{\xi}_1$	Right turn $\bar{\xi}_2$	St. line $\bar{\xi}_3$	Target St. line $\bar{\xi}_4$	Left turn \bar{t}_1	Right turn \bar{t}_2	St. line \bar{t}_3	Target St. line \bar{t}_4	Total value f	Total value t
Optimal Path	0	1.07	5.75	2.73	0	0.21	1.15	1.36	9.55	1.36
Feasible Path	5.65	0	6.63	4.91	1.13	0	1.33	2.46	17.19	2.46

We further evaluated the adaptability of Algorithm (5.1) by conducting tests in various directions, including scenarios where the target travels horizontally relative to the pursuer. The analysis for these scenarios is presented in Figure 5(a)(b) and data summarized in Table 3, considering an initial position for $P(0, 0, \pi/3)$ and $T(8, 3, \pi)$.

In addition, we tested our proposed model (28) for larger turning radius $R = 3$ and various target directions which demonstrated in Figure 6(a)(b) and detailed of the results depicted in Table 4, maintaining the pursuer and target positions at $P(0, 0, \pi/3)$ and $T(8, 3, \pi)$, and also for the pair $P(0, 0, \pi/3)$ and $T(-1, 10, 3\pi/2)$.

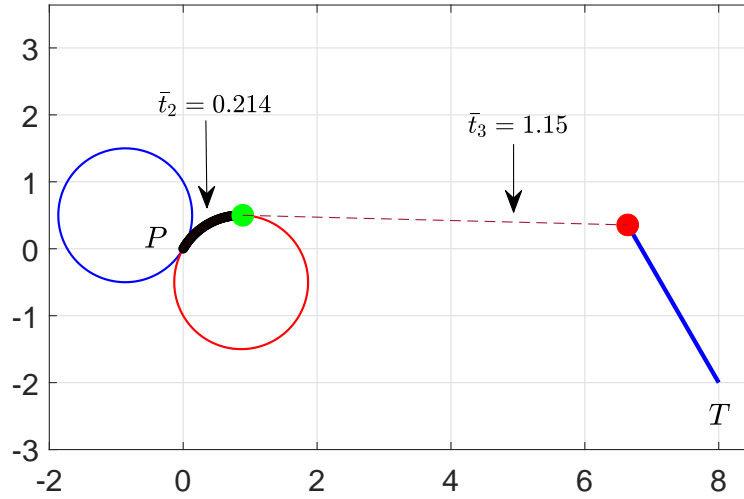


(a) Optimal path.

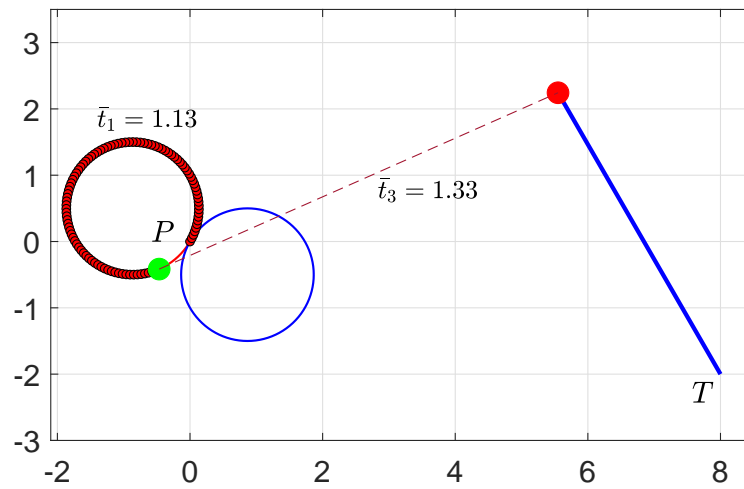


(b) Feasible path.

Figure 3: Optimizing the path of the pursuer, starting at position $P(0,0)$ with a heading angle of $\theta_P = 2\pi/3$, to intercept target $T(-5,0)$, which is located to the left of the pursuer and heading in the direction of $\theta_T = \pi/2$.

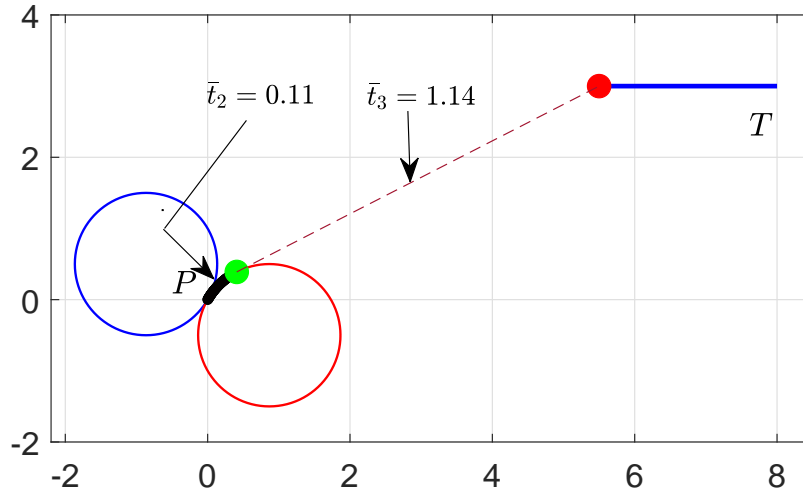


(a) Optimal path.

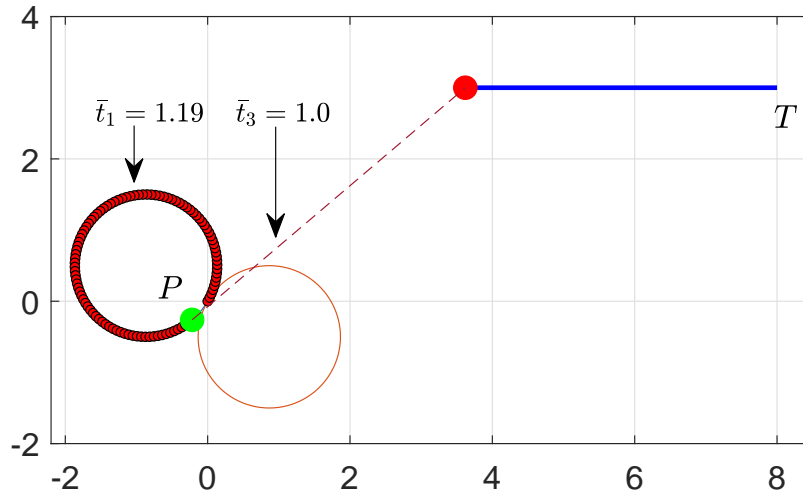


(b) Feasible path.

Figure 4: Optimizing the path of the pursuer, starting at position $P(0,0)$ with a heading angle of $\theta_P = \pi/3$, to intercept target $T(8, -2)$, which is located to the right of the pursuer and heading in the direction of $\theta_T = 2\pi/3$.

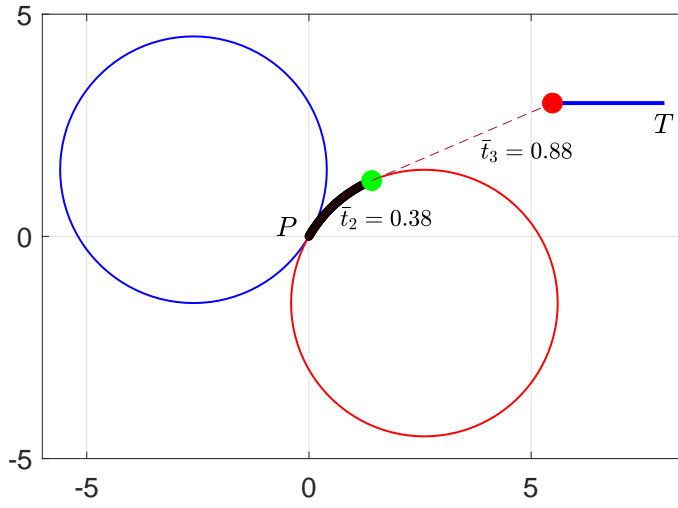


(a) Optimal path.

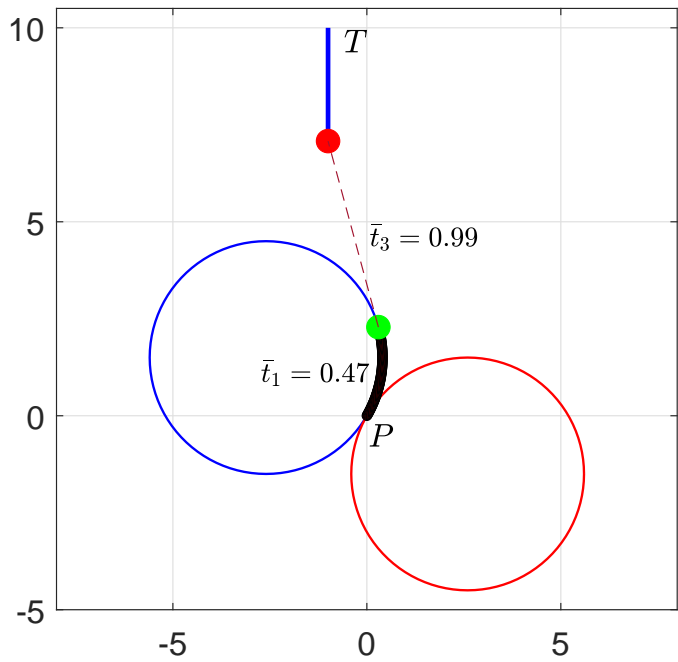


(b) Feasible path.

Figure 5: Optimizing the path of the pursuer, starting at position $P(0,0)$ with a heading angle of $\theta_P = \pi/3$, to intercept target $T(8,3)$, which is located to the right of the pursuer and heading in the direction of $\theta_T = \pi$.



(a) Optimal path for pursuer $P(0, 0, \pi/3)$ and target $T(8, 3, \pi)$.



(b) Optimal path for pursuer $P(0, 0, \pi/3)$ and target $T(-1, 10, 3\pi/2)$.

Figure 6: Optimizing pursuer's path: exploring different target directions with radius $R = 3$.

Table 3: Model Performance Variations for Optimal Path Generations.

$ \mathbf{V} - R$	Length				Time				Total value f	Total value t
	Left turn $\bar{\xi}_1$	Right turn $\bar{\xi}_2$	St. line $\bar{\xi}_3$	Target St. line $\bar{\xi}_4$	Left turn \bar{t}_1	Right turn \bar{t}_2	St. line \bar{t}_3	Target St. line \bar{t}_4		
$ \mathbf{V}_P = 5$ $ \mathbf{V}_T = 2$ $R = 1$										
Optimal Path	0	0.57	5.71	2.51	0	0.11	1.14	1.26	8.80	1.26
Feasible Path	5.94	0	5.03	4.39	1.19	0	1.00	2.20	15.36	2.20

Table 4: Model Performance Variations for Optimal Path Generations.

$ \mathbf{V} - R$	Length				Time				Optimal	
	Left turn $\bar{\xi}_1$	Right turn $\bar{\xi}_2$	St. line $\bar{\xi}_3$	Target St. line $\bar{\xi}_4$	Left turn \bar{t}_1	Right turn \bar{t}_2	St. line \bar{t}_3	Target St. line \bar{t}_4	Total value f	Total value t
$ \mathbf{V}_P = 5$ $ \mathbf{V}_T = 2$ $R = 3$										
$P(0,0) \rightarrow T(8,3)$	0	1.92	4.41	2.53	0	0.38	0.88	1.27	8.87	1.27
$P(0,0) \rightarrow T(-1,10)$	2.37	0	4.96	2.93	0.47	0	0.99	1.46	10.25	1.46

Remark 6.1 In our analysis, we aim to optimize the total physical distance travelled by both the pursuer and the target. However, we can also consider optimizing the time, focusing on reaching the interception of the target as quickly as possible. It's important to note that these two objectives don't always align, especially when acceleration is involved along the path. In our current model, we assume that both the pursuer and the target move with constant velocity. In this context, optimizing the length or optimizing the time both give us the same outcome.

6.1 Special Cases

The turning radius of pursuer depends on both its angular speed (the rate at which it turns or rotates) and its linear speed (its speed in a tangent line). Specifically, the turning radius can be calculated using the relation $R = \frac{|\mathbf{V}|}{|\dot{\theta}(t)|}$ where $|\mathbf{V}|$ is linear speed and $|\dot{\theta}(t)|$ is angular speed. A higher angular velocity (faster turn) or a lower linear velocity (slower straight-line speed) will result in a smaller turning radius, meaning the object or vehicle can make a tighter turn. Conversely, a lower angular velocity or a higher linear velocity will result in a larger turning radius, requiring a wider turn. Keeping this mind we do further analysis of Algorithm (5.1) through the Example-2.

Example 2

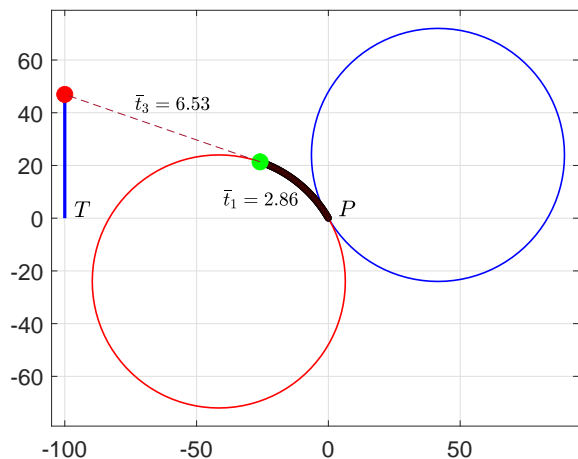
Let an initial position for the pursuer, denoted as $P(0,0,2\pi/3)$ and a target point

$T(-100, 0, \pi/2)$. The objective is for pursuer P with a constant speed $|\mathbf{V}_P|$ to intercept target T has constant speed $|\mathbf{V}_T|$ by obtaining a minimum path f chosen by (28). Now we consider a combination of angular speeds: $|\dot{\theta}(t)| < 1$, $|\dot{\theta}(t)| = 1$, and $|\dot{\theta}(t)| > 1$, with a fixed linear pursuer speed $|\mathbf{V}_P| = 12$. Based on these parameters mentioned above, the turning radius R is calculated using the relation $R = \frac{|\mathbf{V}|}{|\dot{\theta}(t)|}$,

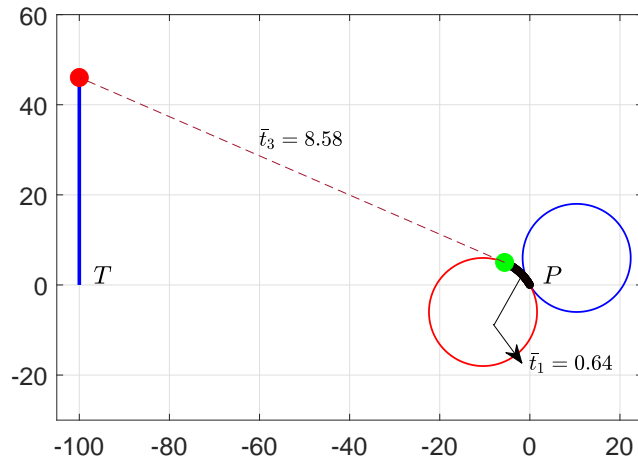
and optimal paths are obtained by model (28) which depicted in Figure 7. We observe that when $|\dot{\theta}(t)| < 1$, the turning radius is $R = 48$, and the optimal path length $f = 159.65$ is achieved, covering one-third of the total length with the turning curve. Conversely, when $|\dot{\theta}(t)| > 1$, the turning radius is $R = 3$, and the optimal path length $f = 156.04$ occurs when the pursuer turns left, but only 1/100 of the total length is covered by the turning curve. These results are tabulated in Table 5, and the optimal paths for these different combinations can be seen in Figure 7. Overall, it appears that improved results are obtained when angular velocity is increased, resulting in a smaller turning radius.

Table 5: *Model Performance Variations with Changing Angular Speed $|\dot{\theta}(t)|$.*

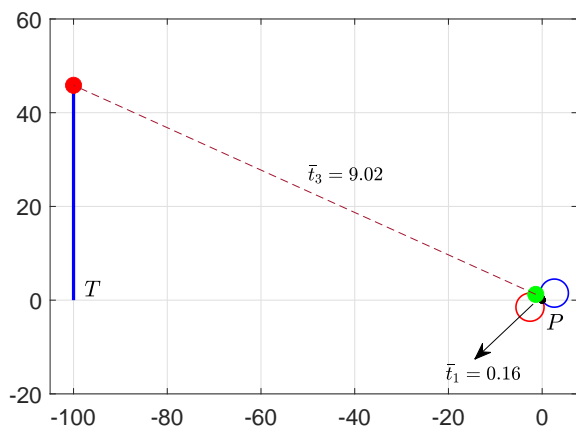
$ \mathbf{V}_P - \dot{\theta}(t) - R$	Length				Time				Optimal	
$ \mathbf{V}_P = 12$ $R = \mathbf{V}_P / \dot{\theta}(t) $	Left turn $\bar{\xi}_1$	Right turn $\bar{\xi}_2$	St. line $\bar{\xi}_3$	Target St. line $\bar{\xi}_4$	Left turn \bar{t}_1	Right turn \bar{t}_2	St. line \bar{t}_3	Target St. line \bar{t}_4	Total value f	Total value t
$ \dot{\theta}(t) = 1/4 \mid R = 48$	34.31	0	78.39	46.96	2.86	0	6.53	9.39	159.65	9.39
$ \dot{\theta}(t) = 1/1 \mid R = 12$	7.64	0	102.94	46.08	0.64	0	8.58	9.22	156.66	9.22
$ \dot{\theta}(t) = 4/1 \mid R = 3$	1.87	0	108.28	45.89	0.16	0	9.02	9.18	156.04	9.18



(a) Optimal path when $|\dot{\theta}(t)| < 1$ and $|\mathbf{V}_P| = 12$.



(b) Optimal path when $|\dot{\theta}(t)| = 1$ and $|\mathbf{V}_P| = 12$.



(c) Optimal path when $|\dot{\theta}(t)| > 1$ and $|\mathbf{V}_P| = 12$.

Figure 7: Optimizing the path of the pursuer, starting at position $P(0,0)$ with a heading angle of $\theta_P = 2\pi/3$, to intercept target $T(-100,0)$, which is located to the left of the pursuer and heading in the direction of $\theta_T = \pi/2$.

7 Conclusion

In this paper, our study presented a robust and efficient approach for determining the shortest path for a pursuer intercepting a moving target with constant speed. Using Dubin's path concepts, our proposed mathematical model combined circular curves and straight-line segments to minimize pursuer lengths or interception time. We established the model's effectiveness in diverse positions of target and pursuer by developing an efficient algorithm and conducting extensive numerical experiments. Our model demonstrated a high convergence rate to approximate solutions, ensuring less computational time.

While our study has made significant progress, there remain intriguing avenues for further exploration in this field. Several questions remain open for future research: One can investigate

- How does the model perform when the target's speed and direction change dynamically? Adapting the model for dynamic targets could enhance its applicability in real-world settings.
- How can the model be extended to incorporate obstacle avoidance strategies? Introducing fixed obstacles in the pursuit scenario could present complex challenges that warrant exploration.
- How does the model behave in scenarios involving multiple pursuers and targets? Investigating the interaction and coordination of multiple objects in pursuit situations could provide valuable insights.

Addressing these open questions can further enhance the adaptability and applicability of our proposed model, paving the way for more sophisticated and effective pursuit strategies in diverse real-world scenarios.

Acknowledgments: M. Akter would like to express her gratitude to Ministry of Science & Technology, Bangladesh for providing financial help in the form of NST fellowship with Reference no. 120005100-3821117, Reg. no. 6 & Session: 2022-2023.

Moreover, we acknowledge Chatgpt(3.5) AI tools which is used to rephrase, edit and polish the authors written text for spelling, grammar, or general style.

References

- [1] Dubins, L. E. (1957). On curves of minimal length with a constraint on average curvature, and with prescribed initial and terminal positions and tangents. *American Journal of mathematics*, 79(3), 497-516.
- [2] Reeds, J., & Shepp, L. (1990). Optimal paths for a car that goes both forwards and backwards. *Pacific journal of mathematics*, 145(2), 367-393.
- [3] Ayala, J., Kirszenblat, D., & Rubinstein, J. H. (2014). A geometric approach to shortest bounded curvature paths. *arXiv preprint arXiv:1403.4899*.
- [4] Sussmann, H. J., & Tang, G. (1991). Shortest paths for the Reeds-Shepp car: a worked out example of the use of geometric techniques in nonlinear optimal control. *Rutgers Center for Systems and Control Technical Report*, 10, 1-71.
- [5] Boissonnat, J. D., Cerezo, A., & Leblond, J. (1994). Shortest paths of bounded curvature in the plane. *Journal of Intelligent and Robotic Systems*, 11, 5-20.
- [6] Bui, X. N., Boissonnat, J. D., Soueres, P., & Laumond, J. P. (1994). Shortest path synthesis for Dubins non-holonomic robot. In *Proceedings of the 1994 IEEE International Conference on Robotics and Automation*, 2-7.
- [7] Chitsaz, H., & LaValle, S. M. (2007). Time-optimal paths for a Dubins airplane. In *2007 46th IEEE conference on decision and control*, 2379-2384.
- [8] Jha, B., Chen, Z., & Shima, T. (2020). On shortest Dubins path via a circular boundary. *Automatica*, 121, 109192.
- [9] Manyam, S. G., Casbeer, D., Von Moll, A. L., & Fuchs, Z. (2019). Shortest Dubins path to a circle. In *AIAA scitech 2019 forum*, 919.
- [10] Chen, Z., & Shima, T. (2019). Shortest Dubins paths through three points. *Automatica*, 105, 368-375.
- [11] Chen, Z. (2020). On Dubins paths to a circle. *Automatica*, 117, 108996.

- [12] Pontryagin, L. S., Boltyanskii, V.G, Gamkrelidze, R. V., & Mishchenko, E. F. (1962) The mathematical theory of optimal processes (Russian), John Wiley and Sons, Interscience Publishers, New York.
- [13] Matveev, A. S., Teimoori, H., & Savkin, A. V. (2011). A method for guidance and control of an autonomous vehicle in problems of border patrolling and obstacle avoidance. *Automatica*, 47(3), 515-524.
- [14] Matveev, A. S., Teimoori, H., & Savkin, A. V. (2012). Method for tracking of environmental level sets by a unicycle-like vehicle. *Automatica*, 48(9), 2252-2261.
- [15] Gopalan, A., Ratnoo, A., & Ghose, D. (2016). Time-optimal guidance for lateral interception of moving targets. *Journal of Guidance, Control, and Dynamics*, 39(3), 510-525.
- [16] Gopalan, A., Ratnoo, A., & Ghose, D. (2017). Generalized time-optimal impact-angle-constrained interception of moving targets. *Journal of Guidance, Control, and Dynamics*, 40(8), 2115-2120.
- [17] Manyam, S. G., Casbeer, D., Von Moll, A., & Fuchs, Z. (2019). Optimal dubins paths to intercept a moving target on a circle. In 2019 American Control Conference (ACC), 828-834.
- [18] Buzikov, M. E., & Galyaev, A. A. (2021). Time-optimal interception of a moving target by a Dubins car. *Automation and Remote Control*, 82, 745-758.
- [19] Looker, J. R. (2008). Minimum Paths to Interception of a Moving Target when Constrained by Turning Radius.
- [20] Meyer, Y., Isaiah, P., & Shima, T. (2014). On Dubins paths to intercept a moving target at a given time. *IFAC Proceedings Volumes*, 47(3), 2521-2526.
- [21] Meyer, Y., Isaiah, P., & Shima, T. (2015). On Dubins paths to intercept a moving target. *Automatica*, 53, 256-263.
- [22] Kaya, C. Y. (2017). Markov–Dubins path via optimal control theory. *Computational Optimization and Applications*, 68(3), 719-747.
- [23] Kaya, C. Y. (2019). Markov–Dubins interpolating curves. *Computational Optimization and Applications*, 73(2), 647-677.
- [24] Zheng, Y., Chen, Z., Shao, X., & Zhao, W. (2021). Time-optimal guidance for intercepting moving targets by dubins vehicles. *Automatica*, 128, 109557.

- [25] Zheng, Y., Zheng, C. H. E. N., Xueming, S. H. A. O., & Wenjie, Z. H. A. O. (2022). Time-optimal guidance for intercepting moving targets with impact-angle constraints. *Chinese Journal of Aeronautics*, 35(7), 157-167.
- [26] Forkan, M., Rizvi, M. M., & Chowdhury, M. A. M. (2022). Optimal path planning of Unmanned Aerial Vehicles (UAVs) for targets touring: Geometric and arc parameterization approaches. *Plos one*, 17(10), e0276105.
- [27] Hou, L., Luo, H., Shi, H., Shin, H. S., & He, S. (2023). An Optimal Geometrical Guidance Law for Impact Time and Angle Control. *IEEE Transactions on Aerospace and Electronic Systems*.
- [28] Fourer, R., Gay, D. M., & Kernighan, B. W. (2003). *AMPL: A Modeling Language for Mathematical Programming, Second Edition*, Brooks/Cole Publishing Company / Cengage Learning.
- [29] Wächter, A., & Biegler, L. T. (2006). On the implementation of an interior-point filter line-search algorithm for large-scale nonlinear programming. *Mathematical programming*, 106, 25-57.
- [30] Byrd, R. H., Nocedal, J., & Waltz, R. A. (2006). Knitro: An integrated package for nonlinear optimization. *Large-scale nonlinear optimization*, 35-59.